Eccentric MMR with Perturber

JT Laune

July 26, 2021

1 Relevant Background

In this section, we consider a $j : j+1$ MMR between a test particle and a planet of mass μ_p. For the rest of this report, the subscript "p" denotes orbital parameters of the massive planet, no subscript denotes the test particle, and a subscript "ext" denotes an external perturber. The Hamiltonian is given by

$$H = -\frac{1}{2\Lambda^2} \pm \mu_p \left(A \left(\frac{2\Gamma}{\Lambda} \right)^{1/2} \cos\theta + B e_{\rm p} \cos\theta_p \right) - \mu_p \left(C \left(\frac{2\Gamma}{\Lambda} + e_{\rm p}^2 \right) + D e_{\rm p} \sqrt{\frac{2\Gamma}{\Lambda}} \cos\gamma \right) \quad (1)$$

The $(\pm)$ term is $(+)$ for an internal resonance, and $(-)$ for an external resonance. The period ratio α is defined to be a/a_p for an internal resonance, and a_p/a for an outer resonance. A, B, C and D are functions of α, and their definitions are given in A.1 in terms of Laplace coefficients. They are different expressions, values, and signs depending on whether or not the resonance is internal or external.

1.1 Disk forces

The forces the disk exerts on the test particle are given in a parametrized fashion by $T_{\rm e}$, the eccentricity damping timescale, and $T_{\rm m}$, the migration timescale:z

$$\frac{\dot{a}}{a} = \pm \frac{1}{T_{\rm m}} - \frac{2e^2}{T_{\rm e}} \quad (2)$$

The $(\pm)$ becomes $(+)$ for outward migration, and $(-)$ for inward migration. The eccentricity damping force is given by

$$\frac{\dot{e}}{e} = -\frac{1}{T_{\rm e}}.$$

We note that $T_{\rm e} > 0$ always.

1.2 Equilibrium eccentricity

In the case of a massive planet on a circular orbit ($e_{\rm p} = 0$), a test particle in mean motion resonance will reach an equilibrium eccentricity depending on the ratio $\sqrt{T_{\rm e}/T_{\rm m}}$.

For an internal resonance, the equilibrium eccentricity is given by

$$e_{\rm disk} = \sqrt{\frac{T_{\rm e}}{2jT_{\rm m}}}$$

For an external resonance, the equilibrium eccentricity is given by

$$e_{\rm disk} = \sqrt{\frac{T_{\rm e}}{2(j+1)T_{\rm m}}}$$

INSERT relating $e_{\rm disk}$ to disk aspect ratio .

1.3 Stability

For both internal and external resonances, the planet must be massive enough to capture the test particle:

$$\mu_{\rm cap}^{4/3} \gg \frac{1}{T_m}.$$

In the case of an external test particle, the resonance is always stable and librations go to zero.

For an internal test particle, stability depends upon the disk parameters and planet mass μ_p:

$$\begin{aligned} \textbf{Stable, no libration}: &\quad \mu_p > \frac{3j^2}{\alpha_0 A} e_{\rm eq}^3 \\ \textbf{Stable, finite libration}: &\quad \frac{3j^2}{\alpha_0 A} e_{\rm eq}^3 > \mu_p > \frac{3j}{8\alpha_0 A} e_{\rm eq}^3 \\ \textbf{Unstable, escape}: &\quad \frac{3j}{8\alpha_0 A} e_{\rm eq}^3 > \mu_p. \end{aligned} \quad (3)$$

1.4 Eccentricity of μ_p

Through a series of canonical transformations, we may combine the $e_{\rm p}$ term of the Hamiltonian with the e term. The transormed Hamiltonian for $e_{\rm p} > 0$ is

$$H = \eta R - R^2 - \sqrt{R}\cos\bar{\theta}.$$

The momentum $R \propto \bar{e}^2$, where $\bar{e}$ is

$$\bar{e}^2 = e^2 + \frac{2B}{A} e e_{\rm p} \cos\gamma + \frac{B^2}{A^2} e_{\rm p}^2.$$

The "shifted" $\overline{\gamma}$ is given by

$$\overline{\gamma} = \tan^{-1}\left(\frac{e\sin\gamma}{e\cos\gamma + Be_p/A}\right)$$

The resonance angle is then given by

$$\theta = (j+1)\lambda_p - j\lambda + \overline{\gamma}$$

for an internal resonance, and

$$\theta = (j+1)\lambda - j\lambda_p + \overline{\gamma}$$

for an external resonance. We will only be utilizing $\bar{e}$ and $\bar{\gamma}$ in this report, but the full details of this are given in A.3 for completeness.

1.5 External Perturber

A massive external companion induces relative apsidal precession within the MMR pair. We use a parametrized approach, by transforming to the rotating frame of γ_p and then setting $\dot{\gamma} = -\omega_{\rm ext}$ with the following Hamiltonian:

$$H_{\gamma,\rm sec} = -\Gamma(\omega_{1,\rm ext} - \omega_{p,\rm ext}) \equiv -\Gamma\omega_{\rm ext}.$$

The units of $\omega_{\rm ext}$ are in $[n_p]$.

An external companion will also induce precession in λ, which we may include with the following Hamiltonian

$$H_{\lambda,\rm sec} = -\frac{GM}{2a_p}\mu_p b^{(0)}_{1/2}\left(\frac{a}{a_p}\right) - \frac{GM}{2a_{\rm ext}}\mu_{\rm ext} b^{(0)}_{1/2}\left(\frac{a}{a_{\rm ext}}\right) - \frac{GM}{2a_{\rm ext}}\mu_{\rm ext} b^{(0)}_{1/2}\left(\frac{a_p}{a_{\rm ext}}\right)$$

We treat $a_{\rm ext}$ as an independent variable, and choose it to be $a_{\rm ext} = 3$ throughout this work. Then, we solve for $\mu_{\rm ext}$ with the following formulas:

$$\omega_{1,\rm ext} = \mu_{\rm ext}\left(\frac{a_p}{a}\right)^{3/2}\frac{a^2}{4a_{\rm ext}^2} b^{(1)}_{3/2}\left(\frac{a}{a_{\rm ext}}\right)$$

$$\omega_{p,\rm ext} = \mu_{\rm ext}\frac{a_p^2}{4a_{\rm ext}^2} b^{(1)}_{3/2}\left(\frac{a_p}{a_{\rm ext}}\right).$$

1.6 Resonance width

The resonance widths in a- and e-space, in units of δn, are given by

$$\frac{\delta a}{a} \sim \frac{\delta n}{n} \sim \mu_p^{2/3}$$

$$\frac{\delta e}{e} \sim \mu_p^{1/3}$$

INSERT derivation or citation

1.7 (WIP) Resonance splitting

INSERT discussion of resonance splitting, etc

2 Summary of Results

See Table 1 for a summary of the integrations carried out in this work. See Table 2 for a compact summary of the regimes explored in this work, as well as our notable results.

3 Unperturbed ($\omega_{\rm ext} = 0$) resonant behavior

3.1 Equilibrium eccentricity

For $e_{\rm disk} > e_p > 0$, the test particle librates around $e_{\rm disk}$, as expected (see the right of Figure 1). Whenever $e_{\rm disk} < e_p$, however, the librations of e_1 are typically large and centered away from $e_{\rm disk}$.

3.2 Apsidal alignment

For the $e_{\rm disk} \lesssim e_{\rm p}$ regime, when the disk forces dominate over the eccentricity of μ_p, $\dot{\gamma} \approx 0$ and $|\gamma - \gamma_p| \approx 0$, resulting in apsidal alignment. In the opposite regime, $\dot{\gamma} \neq 0$ and $|\gamma - \gamma_p|$ circulates. For $e_{\rm disk} \sim e_{\rm p}$ we must turn to numerical simulations to find the boundary between γ-aligned and γ-circulating systems.

3.2.1 External

In Figure 1, we plot our integrations for $e_{\rm disk} = 0.018$ and $e_p = 0.1$ (left, γ-aligned) and $e_p = 0.01$ (right, γ-circulating). Figure 2 summarizes the apsidal alignment results for the case of an external resonance. We have a similar trend of apsidal alignment for $e_{\rm p} \gtrsim e_{\rm eq}$ with γ circulating for the opposite regime. The main difference from the internal case is that for the simulations with $e_{\rm p} = e_{\rm eq}$, γ is no longer aligned with γ_P.

The general behavior of γ may be understood from its equation of motion in an external resonance (see A.2):

$$\dot{\gamma} = \mu_p\left(\frac{-A\cos\theta}{\sqrt{2\Gamma\Lambda}} - \frac{2C}{\Lambda} - De_{\rm p}\frac{\cos\gamma}{\sqrt{2\Gamma\Lambda}}\right)$$

where

$$\theta = (j+1)\lambda - j\lambda_p + \gamma$$

is the old resonance angle. We have

$$-A\cos\theta\sqrt{2\Gamma\Lambda} \propto \frac{1}{e}$$

Regime	$e_{\rm disk}$	e_p	$\omega_{\rm ext}$	# runs	Figures
External					
γ-alignment	[0.01,0.1]	[0.01,0.1]	0	25	1,2
external precession	[0.01,0.1]	[0.01,0.1]	[0.1,10]δn	250	4,6,5
Internal					
γ-alignment	[0.01,0.1]	[0.01,0.1]	0	15	3

Table 1: Summary of the integrations carried out in this work. N-body simulations are not included, as they are a WIP. The eccentricities are 5 values distributed equally in log space, and the external precession rates are 10 values distributed the same.

	Internal	**External**			
	$\omega_{\rm ext}=0$	$\omega_{\rm ext}=0$	$\omega_{\rm ext}<\delta n$	$\omega_{\rm ext}\approx\delta n$	$\omega_{\rm ext}>\delta n$
$e_p=0$			unchanged from $\omega_{\rm ext}=0$	unchanged from $\omega_{\rm ext}=0$	unchanged from $\omega_{\rm ext}=0$
$e_{\rm disk}<e_{\rm p}$		γ-aligned	unchanged from $\omega_{\rm ext}=0$	γ-anti-aligned e_1 excited	γ-anti-aligned e_1 suppressed
$e_{\rm disk}\approx e_{\rm p}$	γ-aligned	γ-circulating	unchanged from $\omega_{\rm ext}=0$	chaotic	γ-anti-aligned e_1 suppressed
$e_{\rm disk}>e_{\rm p}$	γ-circulating	γ-circulating	unchanged from $\omega_{\rm ext}=0$	γ-anti-aligned e_1 excited	unclear trend

Table 2: Summary of the results from this study for γ-alignment and eccentricity suppression/excitation. In the case of **"unclear trend"**, the behavior varies between [γ-circulating] and [γ-anti-aligned, e_1 excited]. **"Chaotic"** means that, for closely spaced starting locations a_0 and holding all other conditions equal, the behaviors of γ_1 and e_1 varied between [γ-circulating] and [γ-anti-aligned, e_1 excited]. The results presented here for $\omega_{\rm ext}=0$ are summarizing the plots in Figures 2 and 3. For $\omega_{\rm ext}>0$, they are summarizing the plots in Figure 6. We note that these are a general summary of the results, and sometimes there are exceptions (e.g., for $e_p=e_{\rm disk}=0.01$ and $\omega_{\rm ext}\approx\delta n$, the runs are not [$\gamma$-anti-aligned, e_1 excited], see the leftmost plot in Figure 6).

$$-\frac{2C}{\Lambda}\propto\mathcal{O}(1)$$
$$-De_{\rm p}\left(\frac{\cos\gamma}{\sqrt{2\Gamma\Lambda}}\right)\sim\mathcal{O}(1)$$

and so the first term typically dominates the motion if $\theta\neq\pi/2$

The shifted resonance angle, however, is

$$\overline{\theta}=(j+1)\lambda-j\lambda_p+\overline{\gamma}$$

where

$$\overline{\gamma}=\tan^{-1}\left(\frac{e\sin\gamma}{e\cos\gamma+Be_{\rm p}/A}\right)$$

When $e_{\rm p}\lesssim e_{\rm eq}$, $\gamma\approx\overline{\gamma}$ and $\theta\to0$, meaning the first term will dominate $\dot{\gamma}$. However, when $e_{\rm p}\gtrsim e_{\rm eq}$, θ circulates and the first term averages to 0, leading to the second two terms governing the equation of motion. For these two terms, if $e_{\rm p}\gtrsim e_{\rm eq}$, an equilibrium exists where $\dot{\gamma}\to0$ for $\gamma\to0$.

The behavior of $\dot{\gamma}$ and its individual components along with the corresponding behavior of $\gamma,\theta,\overline{\theta}$ is plotted in Figure 4. From the left column to the right, we hold $e_{\rm disk}=0.03$ and increase $e_{\rm p}$ uniformly in log-space between 0.01 and 0.1. We can see that between the third and fourth columns, at the transition between apsidal circulation and alignment, θ begins to circulate, and vice versa. Note that $\overline{\theta}\to\pi$ always, as it should in resonance.

3.2.2 Internal

The situation for an internal resonance is similar: if $e_{\rm disk}\sim e_{\rm p}$, then $|\gamma-\gamma_p|$ librates around 0. If $e_{\rm disk}>e_{\rm p}$, then $|\gamma-\gamma_p|$ circulates. If $e_{\rm disk}<e_{\rm p}$ (bot-

Figure 1:

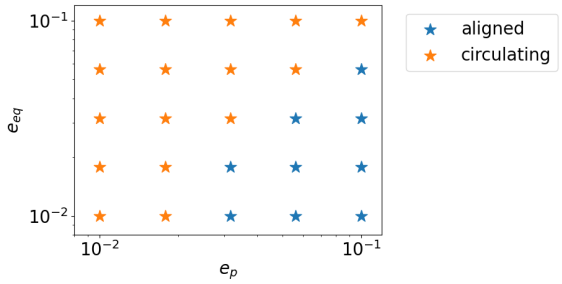

Figure 2:

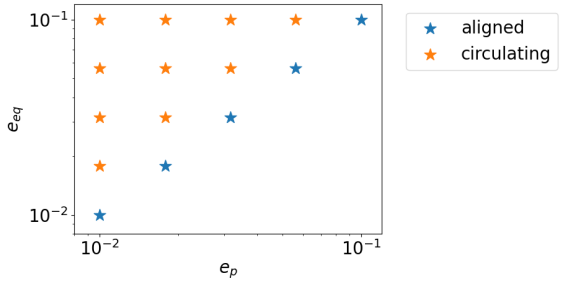

Figure 3:

tom right triangle of Figure 3), the test particle is not captured into resonance (i.e., $\bar{\theta}$ circulates) or equation (2) breaks down and the particle migrates in the opposite direction. This is a limitation of our migration model and is not necessarily physical. Our simulation results have been compiled into Figure 3. For these simulations, μ_p was chosen to be $\mu_p = 1.5 \times \mu_{\rm stable}$, where $\mu_{\rm stable}$ is given in the top line of equations (3).

3.2.3 Non-chaotic transition

In Figure 2, the boundary between the apsidally aligned and anti-aligned regions is sharp up to a precision of 2×10^{-3} in eccentricity space.

To test this, we performed simulations with initial conditions matching the simulation in the center of the grid ($e_{\rm p} = 0.032$, $e_{\rm disk} = 0.032$). From there, we tested simulations moving down on the grid (i.e., holding $e_{\rm disk}$ constant and decreasing $e_{\rm p}$) and moving right on the grid (i.e., holding $e_{\rm p}$ constant and $e_{\rm disk}$). These preliminary results have determined the transition happens in the following intervals:

1. For $e_{\rm p} = 0.032$ constant, transition occurs within the interval $e_{\rm disk} \in (0.054, 0.056)$.

2. For $e_{\rm disk} = 0.032$ constant, transition occurs within the interval $e_{\rm p} \in (0.017, 0.018)$.

3.2.4 (WIP) Comparable mass results

3.2.5 (WIP) N-body results

4 Perturbed resonant behavior

Note that we have not performed simulations of an internal MMR perturbed by a giant companion. Thus far, we have observed no disruption of MMR capture due to an induced precession $\omega_{\rm ext}$.

4.1 Circular case $e_p = 0$

For disk conditions ranging between

$$e_{\rm disk} \in [0.01, 0.1],$$

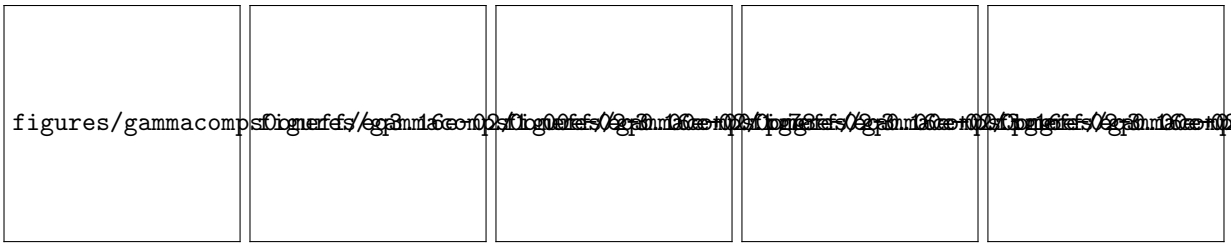

Figure 4:

and external precession frequencies

$$\omega_{\text{ext}} \in [0.1, 10] \times \delta n,$$

we have found no change in resonance for $\mu_p = 10^{-4}$ whenever $e_p = 0$.

4.2 Eccentric case $e_p > 0$

For $\omega_{\text{ext}} < \delta n$, the resonance behavior is largely unchanged.

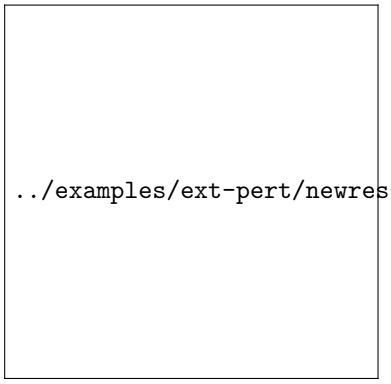

Figure 5:

However, for $\omega_{\text{ext}} \sim \delta n$, a new behavior is observed: $\gamma \to \pi$ and the resonance becomes anti-aligned. In Figure 5, we have plotted an integration for $e_{\text{disk}} = 0.032$, $e_p = 0.1$ to demonstrate this behavior. In addition to this, the average eccentricity e_1 is excited to higher values.

For $\omega_{\text{ext}} > \delta n$, depending on the relationship between e_{disk} and e_{p}, e_1 may be suppressed to small values, while $\gamma \to \pi$ and the apsidal anti-alignment remains. For $e_{\text{p}} > e_{\text{disk}}$, the values of e_1 decrease below e_{disk} as ω_{ext} increases. For $e_{\text{p}} \lesssim e_{\text{disk}}$, occasionally e_1 "breaks" out of the trend to return to $\sim e_{\text{disk}}$.

This can be understood from the equation of motion for γ (see A.2), where we have added the external precession frequency ω_{ext} (see 1.5). In case of γ circulating:

$$-\mu_p\left(\frac{A\cos\theta}{\Lambda e} + \frac{2C}{\Lambda} + \frac{De_p\cos\gamma}{\Lambda e} + \frac{\omega_{\text{eff}}}{\mu_p}\right) > 0$$

$$\Rightarrow \frac{1}{e\Lambda}(A + De_p|\langle\cos\gamma\rangle|) > \frac{2C}{\Lambda} + \frac{\omega_{\text{eff}}}{\mu_p}$$

In case of γ locked:

$$-\mu_p\left(\frac{A\cos\theta}{\Lambda e} + \frac{2C}{\Lambda} + \frac{De_p\cos\gamma}{\Lambda e} + \frac{\omega_{\text{eff}}}{\mu_p}\right) \approx 0$$

$$\Rightarrow \frac{1}{e\Lambda}(A + De_p|\langle\cos\gamma\rangle|) \approx \frac{2C}{\Lambda} + \frac{\omega_{\text{eff}}}{\mu_p}$$

These results are summarized by the series of plots in Figure 6.

4.2.1 (WIP) Phase diagrams

See Figure 7 for preliminary results.

4.2.2 (WIP) Comparable mass results

WIP, code written, not working/tested yet.

4.2.3 (WIP) N-body results

See Figure 8 for preliminary results.

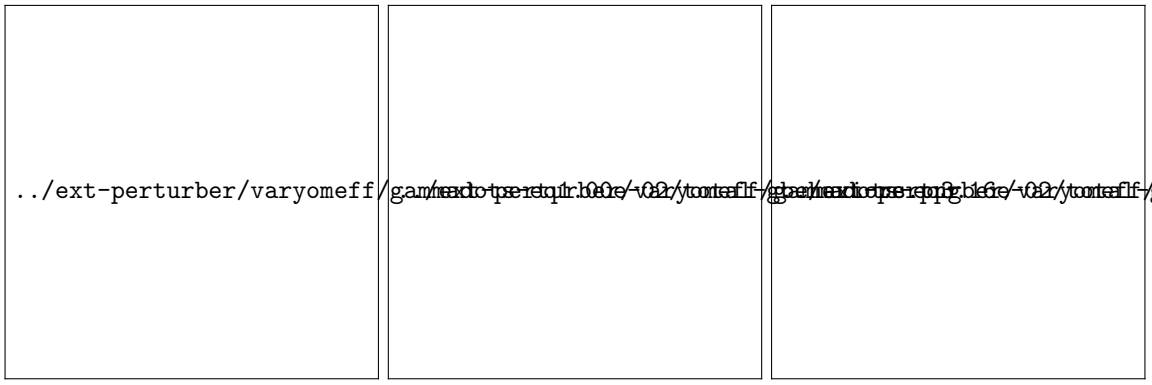

Figure 6:

Figure 7:


../nbody/testsuite/collect/precess-eq1.00e-02ep1.00e-01/m1.00e-03.png
../nbody/testsuite/collect/precess-eq1.00e-02ep1.00e-01/m1.00e-02.png

Figure 8:

A Appendix

A.1 Resonant coefficients

The coefficients for an internal resonance are:

$$A = \frac{1}{2}[2(j+1) + \alpha D]b_{1/2}^{(j+1)}(\alpha) \approx 2.0$$
$$B = -\frac{1}{2}[-1 + 2(j+1) + \alpha D]b_{1/2}^{(j)}(\alpha) \approx -2.5$$
$$C = \frac{1}{8}[2\alpha D + \alpha^2 D^2]b_{1/2}^{(0)}(\alpha) \approx 1.15$$
$$D = \frac{1}{4}[2 - 2\alpha D - \alpha^2 D^2]b_{1/2}^{(1)}(\alpha) \approx -2.0,$$

where $b_k^{(j)}$ are the usual Laplace coefficients (e.g. Murray & Dermott 2000). For an external resonance:

$$A = \frac{1}{2}\alpha[-1 + 2(j+1) + \alpha D]b_{1/2}^{(j)}(\alpha) \approx 1.9$$
$$B = -\frac{1}{2}\alpha[2(j+1) + \alpha D]b_{1/2}^{(j+1)}(\alpha) \approx -1.5$$
$$C = \frac{1}{8}\alpha[2\alpha D + \alpha^2 D^2]b_{1/2}^{(0)}(\alpha) \approx 0.9$$
$$D = \frac{1}{4}\alpha[2 - 2\alpha D - \alpha^2 D^2]b_{1/2}^{(1)}(\alpha) \approx -1.5.$$

A.2 Equations of Motion

The full equations of motion, derived from the Hamiltonian in equation 1, for an internal resonance, are given by:

$$H = -\frac{1}{2\Lambda^2} + \mu_p \left(A \left(\frac{2\Gamma}{\Lambda} \right)^{1/2} \cos\theta + Be_p \cos\theta_p \right) - \mu_p \left(C \left(\frac{2\Gamma}{\Lambda} + e_p^2 \right) + De_p \sqrt{\frac{2\Gamma}{\Lambda}} \cos\gamma \right)$$

$$\dot{\lambda} = \frac{1}{\Lambda^3} + \mu_p \left(-A\sqrt{\frac{\Gamma}{2\Lambda^3}} \cos\theta + C\frac{2\Gamma}{\Lambda^2} + De_p \sqrt{\frac{\Gamma}{2\Lambda^3}} \cos\gamma \right)$$
$$\dot{\Lambda} = -\mu_p \left(Aj\sqrt{\frac{2\Gamma}{\Lambda}} \sin\theta + Bje_p \sin\theta_p \right) + \frac{\Lambda}{2}\left(\frac{1}{T_m} - \frac{4\Gamma}{\Lambda T_e} \right)$$
$$\dot{\gamma} = \mu_p \left(\frac{A\cos\theta}{\sqrt{2\Gamma\Lambda}} - \frac{2C}{\Lambda} - De_p \frac{\cos\gamma}{\sqrt{2\Gamma\Lambda}} \right)$$
$$\dot{\Gamma} = \mu_p \left(A\sqrt{\frac{2\Gamma}{\Lambda}} \sin\theta - De_p \sqrt{\frac{2\Gamma}{\Lambda}} \sin\gamma \right) - \frac{\Gamma}{\Lambda}\frac{\Lambda}{2}\left(\frac{1}{T_m} - \frac{4\Gamma}{\Lambda T_e} \right) - \frac{2\Gamma}{T_e}$$

For an external resonance, are given by:

$$H = -\frac{1}{2\Lambda^2} - \mu_p \left(A \left(\frac{2\Gamma}{\Lambda} \right)^{1/2} \cos\theta + Be_p \cos\theta_p \right) - \mu_p \left(C \left(\frac{2\Gamma}{\Lambda} + e_p^2 \right) + De_p \sqrt{\frac{2\Gamma}{\Lambda}} \cos\gamma \right)$$

$$
\begin{aligned}
\dot{\lambda} =& \frac{1}{\Lambda^3} + \mu_p \left(A\sqrt{\frac{\Gamma}{2\Lambda^3}} \cos\theta + C\frac{2\Gamma}{\Lambda^2} + De_p\sqrt{\frac{\Gamma}{2\Lambda^3}} \cos\gamma \right) \\
\dot{\Lambda} =& \mu_p \left(Aj\sqrt{\frac{2\Gamma}{\Lambda}} \sin\theta B j e_p \sin\theta_p \right) + \frac{\Lambda}{2} \left(-\frac{1}{T_m} - \frac{4\Gamma}{\Lambda T_e} \right) \\
\dot{\gamma} =& \mu_p \left(\frac{-A\cos\theta}{\sqrt{2\Gamma\Lambda}} - \frac{2C}{\Lambda} - De_p \frac{\cos\gamma}{\sqrt{2\Gamma\Lambda}} \right) \\
\dot{\Gamma} =& \mu_p \left(-A\sqrt{\frac{2\Gamma}{\Lambda}} \sin\theta - De_p\sqrt{\frac{2\Gamma}{\Lambda}} \sin\gamma \right) \\
& - \frac{\Gamma}{\Lambda}\frac{\Lambda}{2} \left(-\frac{1}{T_m} - \frac{4\Gamma}{\Lambda T_e} \right) - \frac{2\Gamma}{T_e}
\end{aligned}
$$

A.3 Reduced Hamiltonian

The reduced Hamiltonian for an internal resonance with $e_{\mathrm{p}} > 0$ is given by:

$$
\begin{aligned}
\overline{\Gamma} &= \Gamma + \frac{\sqrt{\Lambda_0}B}{A} e_p \sqrt{2\Gamma} \cos\gamma + \frac{\Lambda_0 B^2}{A^2} e_p^2 \\
\overline{\gamma} &= \tan^{-1}\left(\frac{e\sin\gamma}{e\cos\gamma + Be_p/A} \right) \\
\overline{e}^2 &= e^2 + \frac{2B}{A} e_p e\cos\gamma + \frac{B^2}{A^2} e_p^2 \\
\overline{\theta} &= (j+1)\lambda_p - j\lambda + \overline{\gamma} \\
\overline{H} &= -\frac{(GM)^2}{2\Lambda^2} + \frac{Gm_p}{a_p} A\sqrt{\frac{2\overline{\Gamma}}{\Lambda}} \cos\overline{\theta},
\end{aligned}
$$

and in the external case:

$$
\begin{aligned}
\overline{\Gamma} &= \Gamma + \frac{\sqrt{\Lambda_0}B}{A} e_p \sqrt{2\Gamma} \cos\gamma + \frac{\Lambda_0 B^2}{A^2} e_p^2 \\
\overline{\gamma} &= \tan^{-1}\left(\frac{e\sin\gamma}{e\cos\gamma + Be_p/A} \right) \\
\overline{e}^2 &= e^2 + \frac{2B}{A} e_p e\cos\gamma + \frac{B^2}{A^2} e_p^2 \\
\overline{\theta} &= (j+1)\lambda - j\lambda_p + \overline{\gamma} \\
\overline{H} &= -\frac{(GM)^2}{2\Lambda^2} - \frac{Gm_p}{a_p} \alpha A\sqrt{\frac{2\overline{\Gamma}}{\Lambda}} \cos\overline{\theta}
\end{aligned}
$$